

ESO Phase 3 Data Release Description

Data Collection	VIDEO_CDFS
Release Number	2
Data Provider	Matt Jarvis
Date	02.02.2015

Abstract

VIDEO is a deep near-infrared survey which targets ~ 12 square degrees over the ELAIS-S1, XMM-LSS, and ECDFS extragalactic fields. This document describes the release of the deep stacked data in the VIDEO-CDFS area in Z,J,H and Ks bands. To the 5σ limit, our Ks-band selected catalogue contains 187,869 unique sources with $K_s < 23.5$ (AB) over $\sim 1.5 \text{ deg}^2$ (in the CDFS1 tile).

Overview of Observations

We release individual stacked paw prints and tiles from 01/10/2010 through to 27/12/2013 and deep-stack images for the VIDEO-CDFS field using data taken from 01/10/2010 through to 01/10/2013. The data taken between 01/10/2013 and 27/12/2013 will be incorporated into the deep-stacks in the next data release. These data have all been reprocessed using v1.3 of the VISTA reduction pipeline. The data includes Z,J,H,Ks deep-stacks and catalogues in the VIDEO-CDFS1 tile, along with J and Ks-band data for CDFS2 and CDFS3. The observing strategy, reduction and photometry for individual tiles, source lists and deep-stack data for the VIDEO survey are fully described in the VIDEO Survey paper (Jarvis et al. 2013).

Release Content

We release individual tile data in Z,J,H and Ks bands over the full ECDFS survey region (Figure 1), along with deep-stacked tiles centred on CDFS1 in Z,J,H,Ks filters and in CDFS2 and CDFS3 in J and Ks filters.

We also provide a Ks-selected catalogue “video_er2_03h30-027d34_zjyhks_finalSourceCat_644245094408.fits” in CDFS1 that provides band-merged photometry using the Ks-band as the detection image, conducting forced photometry on the shorter wavelength imaging data, which contains a total of 236,901 unique sources. We recommend using only those sources with $K_s < 23.5$ for most studies as this gives a completeness of ~ 90 per cent (Jarvis et al. 2013), which provides 187,869 unique sources.

In the Ks-selected band-merged catalogue, columns where the value is “NaN” denote that the object was detected at the position of the Ks-band source with negative flux, this occurs over all apertures and filters for different objects, but is mostly a problem for the larger aperture.

In addition to tiles and associated source lists that were released in DR2 we include further tiles in all CDFS tiles. In this release we include stacked individual paw-prints (i.e. paw prints that are made up of the jittered exposures that were used to produce the final deep-stack image for each filter (see Jarvis et al. 2013 for details).

This release therefore provides all stacked paw-prints, single-OB tiles, for all fields, and all have been reprocessed through version 1.3 of the VISTA pipeline and supersede previous releases.

Table 1. Summary of deep-stack image and catalogue release and associated dates of observations which contribute to the release.

Tiles	Deep-stack tile filters/catalogues	Deep-stack tile/catalogues dates	Band-merged catalogue	Band-merged catalogues dates
VIDEO-CDFS1	Z,,H,Ks (no Y)	03/11/2010-27/11/2012	1 merged catalogue: Z,J,H,Ks	03/11/2010-27/11/2012
VIDEO-CDFS2	J,Ks	16/11/2012-29/12/2012	N/A	N/A
VIDEO-CDFS3	J,Ks	21/11/2012-24/01/2013	N/A	N/a

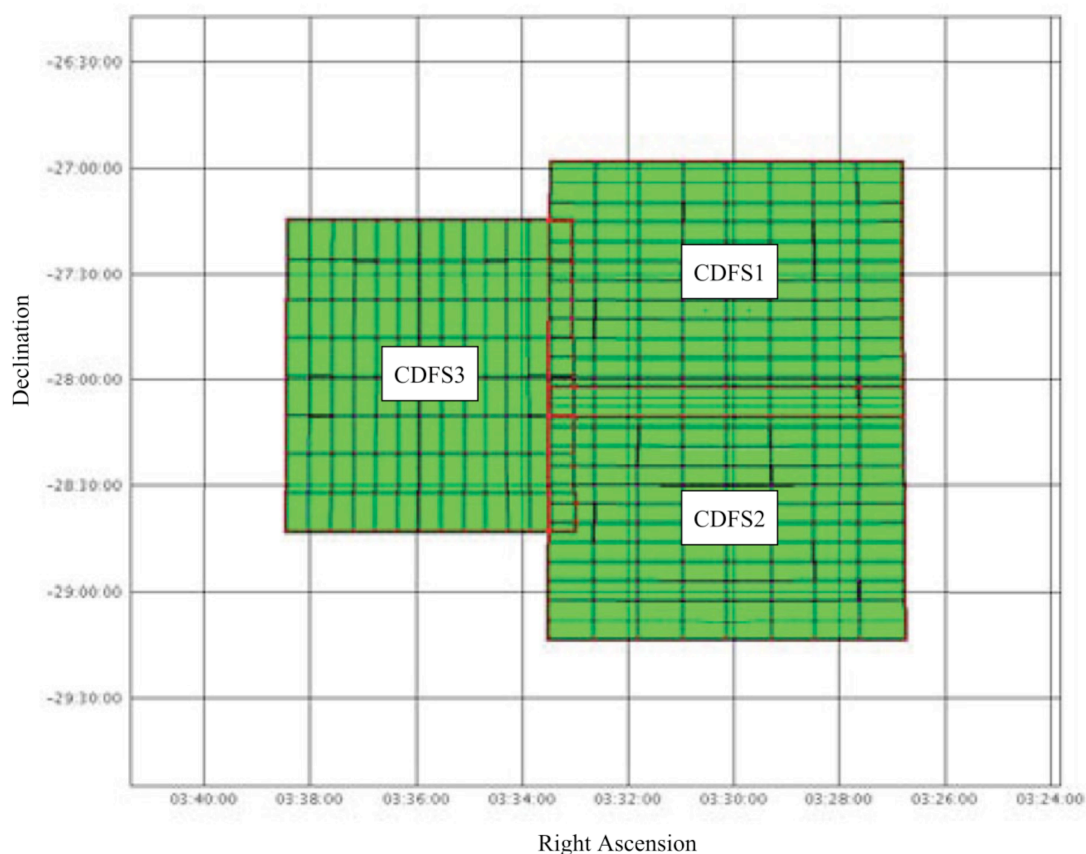


Figure. 1 The coordinates of the VIDEO-CDFS field. This release is comprised of data over all three tiles. Deep stack data are also released over CDFS1, details of which are provided below.

Table 2. Individual paw-prints released, including reprocessed imaging from data release DR2. We note that in a few cases the total exposure time is less than the standard, this due to alteration of survey strategy over the period of observations and the non-completion of some OBs.

Field	Filter	Integration/pixel	Number of paw prints
CDFS-1	Z	500 sec	117
CDFS-1	Z	450 sec	1
CDFS-1	Z	400 sec	2
CDFS-1	Z	350 sec	2
CDFS-1	Z	50 sec	1
CDFS-1	J	480 sec	180
CDFS-1	H	420 sec	129
CDFS-1	H	300 sec	3

CDFS-1	Ks	420 sec	293
CDFS-1	Ks	360 sec	2
CDFS-1	Ks	300 sec	6
CDFS-1	Ks	240 sec	1
CDFS-2	J	480 sec	66
CDFS-2	Ks	420 sec	54
CDFS-3	J	480 sec	70
CDFS-3	J	360 sec	1
CDFS-3	Ks	420 sec	56
CDFS-3	Ks	240 sec	1

Table 3. Individual tiles released, including reprocessed imaging from data release DR2. We note that in a few cases the total exposure time is less than the standard, this due to the non-completion of OBs, we provide details of all of these.

Field	Filter	<i>Integration/tile</i>	<i>Integration/pixel</i>	<i>Number of Tiles</i>
CDFS-1	Z	3000 sec	1000 sec	18
CDFS-1	Z	2900 sec	967 sec	1
CDFS-1	J	2880 sec	960 sec	30
CDFS-1	H	2520 sec	840 sec	20
CDFS-1	H	2400 sec	800 sec	1
CDFS-1	Ks	2520 sec	840 sec	47
CDFS-1	Ks	2340 sec	780 sec	1
CDFS-1	Ks	1800 sec	600 sec	1
CDFS-2	J	2880 sec	960 sec	11
CDFS-2	Ks	2520 sec	840 sec	9
CDFS-3	J	2880 sec	960 sec	11
CDFS-3	Ks	2520 sec	840 sec	9

Table 4. Measured 5σ depths for the VIDEO-CDFS1 deep-stack release in 1-5 arcsec diameter apertures in AB magnitudes. The time given is the total integration time of the paw-prints used to measure these values.

Filter	Time (h) Per pixel	1" (5σ)	2" (5σ)	3" (5σ)	4" (5σ)	5" (5σ)
Z	4.31	25.76	24.76	24.18	23.77	23.44
Y	-	-	-	-	-	-
J	2.67	24.88	23.93	23.38	22.99	22.69
H	3.50	24.38	23.41	22.86	22.46	22.16
Ks	10.28	24.62	23.66	23.10	22.70	22.39

Table 5. Measured 5σ depths for the VIDEO-CDFS2 stack release in 1-5 arcsec diameter apertures in AB magnitudes. The time given is the total integration time of the paw-prints used to measure these values.

Filter	Time (h) Per pixel	1" (5σ)	2" (5σ)	3" (5σ)	4" (5σ)	5" (5σ)
Z	-	-	-	-	-	-
Y	-	-	-	-	-	-
J	2.76	24.79	23.85	23.30	22.91	22.61
H	-	-	-	-	-	-
Ks	2.10	23.76	22.83	22.31	21.93	21.65

Table 6. Measured 5σ depths for the VIDEO-CDFS3 stack release in 1-5 arcsec diameter apertures in AB magnitudes. The time given is the total integration time of the paw-prints used to measure these values.

Filter	Time (h) Per pixel	1" (5σ)	2" (5σ)	3" (5σ)	4" (5σ)	5" (5σ)
Z	-	-	-	-	-	-
Y	-	-	-	-	-	-
J	2.76	24.77	23.83	23.28	22.89	22.58
H	-	-	-	-	-	-
Ks	1.83	23.77	22.79	22.27	21.91	21.62

Release Notes

Data Reduction and Calibration

Initial data reduction steps are performed at the Cambridge Astronomical Survey Unit (CASU) using a software pipeline developed specifically for the reduction of VIRCAM data, as part of the VISTA Data Flow System described by Irwin et al. (2004) and updated on the CASU webpages. This pipeline is modular, and allows different processing recipes to be applied to data obtained with different observing strategies.

For the VIDEO survey, the following steps are applied to each raw data frame (itself the result of NDIR double-correlated- sampling exposures which are co-added by the data acquisition system):

- Destriping – removes a low-level horizontal stripe pattern introduced by the controller and correlates over the four detectors on each controller,
- linearity correction – corrects for the non-linear detector response which is typically 2-4 per cent depending on the detector,
- dark correction – subtracts a mean dark exposure from the image, correcting for dark current and some other electronic effects,
- flat field correction – divides images by a mean twilight sky image, to correct for position-dependent variations in telescope/camera throughput and detector response,
- sky background correction – subtracts an estimate of the atmospheric emission (more details can be found in Jarvis et al. 2013, MNRAS, 428, 1281),
- astrometric calibration – compares the positions of stars in the image with those in the 2MASS point source catalogue (Skrutskie et al. 2006),
- photometric calibration – calculates magnitudes in the VISTA Vega-magnitude photometric system for unsaturated 2MASS stars in the image using their magnitudes and colours in the 2MASS point source catalogue, to set the zero point in the VISTA photometric system, and
- jitter stacking – combines the jittered images in a single paw- print position, using a mean stack of bi-linearly-resampled images, with outlier rejection to remove cosmic rays, fast-moving objects, and bad pixels.

The stacked images provided are based on the paw-print data and use only those paw-print images with <0.9 arcsec seeing. As such parts of completed OBs are not included in the deep stacks, on the other hand some data from aborted OBs are still incorporated in the deep stacks if the individual paw-print met the seeing constraint. Due to the independent data selection for the deep images and the single-OB images, it results for example that the deep co-added images have a total integration time per pixel that is higher than the arithmetic sum of the integration times of the individual Ks tiles.

For the source catalogue:

- Source detection was performed separately for each individual filter. For the deep-stack single-band source lists and the band-merged source catalogue, we carry out the detection and measurement of source photometry using SExtractor (Bertin & Arnouts 1996), with the following parameters (see SExtractor documentation for more information):
- DETECT_MINAREA 3
- THRESH_TYPE RELATIVE
- DETECT_THRESH 3
- ANALYSIS_THRESH 3
- FILTER Y
- FILTER_NAME default.conv
- DEBLEND_NTHRESH 32
- DEBLEND_MINCONT 0.0008
- CLEAN Y
- CLEAN_PARAM 1.0
- MASK_TYPE CORRECT
- PHOT_AUTOPARAMS 2.5, 3.5
- PHOT_PETROPARAMS 2.0, 3.5
- BACK_TYPE AUTO
- BACK_SIZE 64
- BACK_FILTERSIZE 3
- BACKPHOTO_TYPE LOCAL
- BACKPHOTO_THICK 24
- BACK_FILTTHRESH 0.0
- Astrometry is referenced to 2MASS.
- Photometry is performed in the Vega system, and is calibrated by reference to 2MASS stars, using the following colour equations (taken from <http://casu.ast.cam.ac.uk/surveys-projects/vista/technical/photometric-properties>):
- $Z_{\text{VIRCAM}} = J_{2\text{MASS}} + 1.025 \cdot (J-H)_{2\text{MASS}}$
- $Y_{\text{VIRCAM}} = J_{2\text{MASS}} + 0.610 \cdot (J-H)_{2\text{MASS}}$
- $J_{\text{VIRCAM}} = J_{2\text{MASS}} - 0.077 \cdot (J-H)_{2\text{MASS}}$
- $H_{\text{VIRCAM}} = H_{2\text{MASS}} + 0.032 \cdot (J-H)_{2\text{MASS}}$
- $Ks_{\text{VIRCAM}} = Ks_{2\text{MASS}} + 0.010 \cdot (J-Ks)_{2\text{MASS}}$
- The released catalogue are on the AB magnitude system with the following used to convert from Vega to AB.
Z(+0.521), Y(+0.618), J(+0.937), H(+1.384), Ks(+1.839)
- No illumination correction has been applied.
- No correction for extinction has been applied. However, extinction is extremely low for these high-galactic-latitude fields.

For the individual tiles the associated tile-specific source lists are created using the CASU VSA pipeline, details of which can be found at <http://casu.ast.cam.ac.uk/surveys-projects/vista/technical/tiles>

In order to display and analyse the deep-stack images, which are $>2\text{GB}$ then a 64-bit machine is recommended, and all images can be displayed within ds9 for example. If on a machine with less RAM then we recommend using the fitscopy utility within cfitsio, which can be used to extract subsections of the images of interest,

e.g. fitscopy 'filename.fits[x1:x2,y1:y2]' filename.trim.fits

Data Quality

- Astrometric checks have been carried out by comparing with the 2MASS stars within the tiled fields. No systematic offsets are found and the rms scatter is found to be ~ 0.25 arcsec.
- The zero point is uniform across the tile to within the quoted uncertainty (< 0.01 mag).
- Photometry has also been checked against unresolved 2MASS sources within the VIDEO field. We find very good agreement between 2MASS and VIDEO after applying the colour equations to move from the 2MASS system to the VIDEO photometric system.
- The fraction of spurious sources, calculated by inverting the tiled image and re-extracting the sources using the same prescription used for the real extraction, is 0.07 per cent for the Ks-band selected catalogue to the 5sigma depth of 23.7 (2arcsec aperture) in the XMM3 field. Although a similar analysis has not been carried out on the ES1 tiles we expect a similar contamination rate.
- Table 3 in Jarvis et al. (2013) provides the completeness for the various filters over the VIDEO-XMM3 deep-stack. Tables 3,4 and 5 in this document provide similar data for CDFS.

Known issues

Regions of bad pixels in Detector 1 and time varying quantum efficiency in detector 16 renders these detectors the most problematic. The regions of poorer noise statistics are evident in the confidence images. An offset in the photometric calibration of the Y-band data (of the order of 0.1 mag too bright), was an issue in previous releases, this has now been corrected.

Previous Releases

The second public data release of the VIDEO programme via the ESO Science Archive Facility, the VIDEO-ES1 Data Release Number 2, Date: 01.04.2014, contained 40 individual (i.e. single-OB) tile images in the VIDEO-CDFS1 field and their associated single-band source lists. In DR3 we release a total of 159 individual (single-OB) tile images and the associated single-band source lists that have been processed through version 1.3 of the VISTA pipeline. We also release deep-stack images in CDFS1 created from the individual paw-print images that were also processed through v1.3 of the pipeline

Data Format

Files Types

Here we release deep-stacked images and associated aperture matched catalogues. The naming convention for these is:

video_er1_\$POSITION\$_mosaic_\$FILTERNAME\$_deepimage_\$MFID\$.fits.fz

video_er1_\$POSITION\$_mosaic_\$FILTERNAME\$_deepconf_\$MFID\$.fits.fz

video_er1_\$POSITION\$_mosaic_\$FILTERNAME\$_jpeg_\$MFID\$.jpg

video_er1_\$POSITION\$_mosaic_\$FILTERNAME\$_cat_\$MFID\$.fits

where \$POSITION\$ is a string like 03h30-027d34 for the CDFS1 field.

\$FILTERNAME\$ is z,y,j,h,ks AND \$MFID\$ is the multiframeID in our database.

We note that the jpg images are provided for a quick-look at both the science frames and the confidence images.

The single-tile images, confidence maps and source lists have the following naming convention:
v\$DATE\$_\$OBS_NUMBER\$_st_tl.fits.fz

v\$DATE\$_\$OBS_NUMBER\$_st_tl_conf.fits.fz
v\$DATE\$_\$OBS_NUMBER\$_st_tl_cat.fits,
for the tiled image, the confidence image and the source list respectively. \$OBS_NUMBER\$ refers to the final observation number for the individual paw-prints which contribute to the tile.

The paw-print images, confidence maps and source lists have the following naming convention:
v\$DATE\$_\$OBS_NUMBER\$_st.fits.fz
v\$DATE\$_\$OBS_NUMBER\$_st_conf.fits.fz
v\$DATE\$_\$OBS_NUMBER\$_st_cat.fits,
for the tiled image, the confidence image and the source list respectively. \$OBS_NUMBER\$ refers to the final observation number for the individual paw-prints which contribute to the final paw print.

Catalogue Columns

A complete list of catalogue columns for the single-band deep-stack source catalogues is given in Table 6, and Table 7 gives the columns for the Ks-band-selected band-merged catalogue. Table 8 gives the column names of the source catalogues derived from individual single tiles derived using the CASU source extraction pipeline (see <http://casu.ast.cam.ac.uk/surveys-projects/vista/technical/catalogue-generation>).

A brief description of these columns now follows.

Source IDs (ObjID, IAUNAME, SOURCEID)

ObjID gives the unique object identifier for the object in the given filter for this DR1. These identifiers are subject to change in future releases.

IAUNAME is the unique source identifier following the IAU convention, and comprising the survey identifier (“VID”) and then the (truncated) RA and Dec of each object. SOURCEID is the unique source number for the merged catalogue.

Positional Parameters (X, Y, RA, Dec)

X and Y report the position of the object in pixels on the relevant image (which applies to all the stacks, as they share the same coordinate system). RA and Dec (and RA200 and DEC2000 in the merged catalogue) in equinox J2000 are based on the 2MASS astrometric system as described in Jarvis et al. (2013).

Magnitude measurements and errors

Aperture magnitudes are measured in 2” and 5.7” fixed diameter apertures (APERMAGNOAPERCORR3 and APERMAGNOAPERCORR6 columns). We also supply seeing corrected “real” aperture magnitudes for these apertures (APERMAG3 and APERMAG6 columns) that provide the photometry in a seeing convolved 2 and 5.7” aperture. The uncertainties on aperture magnitudes are given in APERMAG3ERR, APERMAG6ERR, APERMAGNOAPERCORR3 and APERMAGNOAPERCORR6. The Petrosian magnitude and the associated error are also provided in columns denoted PETROMAG and PETROMAGERR respectively. SExtractor MAG_AUTO magnitudes and uncertainties are denoted as AUTOMAG and AUTOMAGERR.

To correct for correlated noise in the images, the errors for fixed aperture photometry are estimated by measuring the RMS flux in randomly placed apertures of the same size, then adding Poisson errors based on object counts. Errors for Petrosian fluxes are corrected by scaling the random (non-Poisson) component of the error (as estimated by SExtractor); the scaling factor is estimated by comparing the median SExtractor error for randomly placed 5 arcsec apertures with the actual standard deviation of fluxes in those apertures.

Object flags and source classifier (ERRBITS, CLASSTAT, MERGEDCLASS, HALFRAD, EBV)

The SExtractor flag is provided in the column denoted ERRBITS, indicating if an object is blended or has otherwise corrupted measurements. The best possible object sample are those objects which have ERRBITS = 0.

CLASSTAT gives the SExtractor star/galaxy classification statistic, where 0-galaxy and 1-star. The MERGEDCLASS column in the band-merged catalogue is the weighted average of the individual CLASSTAT parameters for that object.

HALFRAD is the SExtractor measurement of the half-light radius in the given filter.

The galactic reddening E(B-V) is reported at the coordinates of each object in the merged catalogue, computed using the Schlegel et al. (1998) dust maps.

In Jarvis et al. objects were discarded when measuring the completeness and reliability of the catalogues using the HALOFLAG term. This flag does not appear in the released catalogues as such a keyword is subject to interpretation and definition. We encourage potential users of the data to define their own object masks according to their science aims.

Table 7. Complete list of supplied catalogue columns in the deep-stacked single-band catalogues.

Column Number	Column Name	Description
1	OBJID	Unique Source Identifier
2	FILTERID	Filter (1=Z; 2=Y; 3=J; 4=H; 5=Ks)
3	X	X coordinate of detection
4	Y	Y coordinate of detection
5	RA	Right Ascension in Decimal Degrees
6	DEC	Declination in Decimal Degrees
7	APERMAGNOAPERCORR3	Fixed Aperture magnitude (2" diameter", AB)
8	APERMAGNOAPERCORR3ERR	Error in calibrated aperture magnitude 3 (2" diameter", AB)
9	APERMAG3	Aperture magnitude corrected to 2" diameter, AB
10	APERMAG3ERR	Error on Aperture magnitude (2", diameter AB)
11	APERMAGNOAPERCORR6	Fixed Aperture magnitude (5.7" diameter, AB)
12	APERMAGNOAPERCORR6ERR	Error in calibrated aperture magnitude 6 (5.7" diameter", AB)
13	APERMAG6	Aperture magnitude corrected to 5.7" diameter, AB
14	APERMAG6ERR	Error on Aperture magnitude (5.7" diameter), AB
15	AUTOMAG	Extended source magnitude (SExtractor MAG_AUTO)
16	AUTOMAGERR	Extended source mag error (SExtractor MAG_AUTO)
17	HALFRAD	SExtractor Half-light radius
18	PETROMAG	Petrosian Magnitude (AB)
19	PETROMAGERR	Error on Petrosian magnitude
20	ERRBITS	SExtractor Flag
21	CLASSTAT	SExtractor Star/Galaxy classification (0-galaxy, 1-star)

Table 8. Complete list of supplied catalogue columns in the merged video_er2_03h30-027d34_zyhks_finalSourceCat_644245094408.fits. The columns that are reserved for the Y-band data (columns #38 to #52) are dummy columns in this release, and will be populated in subsequent releases when the Y-band data are available.

Column Number	Column Name	Description
1	IAUNAME	IAU-formatted name, prefixed with "VIDEO"
2	SOURCEID	Unique source identifier
3	RA2000	Right Ascension in Decimal Degrees

4	DEC2000	Declination in Decimal Degrees
5	MERGEDCLASS	The average of the CLASSTAT statistic across all bands weighted by $(1/\text{mag_error})^2$
6	EBV	Galactic reddening E(B-V) based on Schegel et al. (1998) dust maps
7	ZMYPNT	Point source colour Z-Y (using aperMag3)
8	ZMYPNTERR	Error on point source colour Z-Y
9	ZMYEXT	Extended source colour Z-Y (using aperMagNoAperCorr3)
10	ZMYEXTERR	Error on extended source colour Z-Y
11	YMJPNT	Point source colour Y-J (using aperMag3)
12	YMJPNTERR	Error on point source colour Y-J
13	YMJEXT	Extended source colour Y-J (using aperMagNoAperCorr3)
14	YMJEXTERR	Error on extended source colour Y-J
15	JMHPNT	Point source colour J-H (using aperMag3)
16	JMHPNTERR	Error on point source colour J-H
17	JMHEXT	Extended source colour J-H (using aperMagNoAperCorr3)
18	JMHEXTERR	Error on extended source colour J-H
19	HMKSPNT	Point source colour H-Ks (using aperMag3)
20	HMKSPNTERR	Error on point source colour H-Ks
21	HMKSEXT	Extended source colour H-Ks (using aperMagNoAperCorr3)
22	HMKSEXTERR	Error on extended source colour H-Ks
23	ZPETROMAG	Z Petrosian magnitude (AB)
24	ZPETROMAGERR	Z Petrosian magnitude error (AB)
25	ZAPERMAG3	Z Aperture magnitude corrected to 2" diameter, AB
26	ZAPERMAG3ERR	Z Error on Aperture magnitude (2", diameter AB)
27	ZAPERMAG6	Z Aperture magnitude corrected to 5.7" diameter, AB
28	ZAPERMAG6ERR	Z Error on Aperture magnitude (5.7" diameter), AB
29	ZAPERMAGNOAPERCORR3	Z Fixed Aperture magnitude (2" diameter", AB)
30	ZAPERMAGNOAPERCORR3ERR	Error in default extended source Z aperture mag, 2.0 arcsec aperture
31	ZAPERMAGNOAPERCORR6	Z Fixed Aperture magnitude (5.7' diameter, AB)
32	ZAPERMAGNOAPERCORR6ERR	Error in extended source Z aperture mag (5.7 arcsec aperture)
33	ZERRBITS	Z SExtractor Flag
34	ZCLASSSTAT	SExtractor Star/Galaxy classification (0-galaxy, 1-star)
35	ZAUTOMAG	Extended source Z mag (SExtractor MAG_AUTO)
36	ZAUTOMAGERR	Extended source Z mag error (SExtractor MAG_AUTO)
37	ZHALFRAD	SExtractor half-light radius in Z band
38	YPETROMAG	Y Petrosian magnitude (AB)
39	YPETROMAGERR	Y Petrosian magnitude error (AB)
40	YAPERMAG3	Y Aperture magnitude corrected to 2" diameter, AB
41	YAPERMAG3ERR	Y Error on Aperture magnitude (2", diameter AB)
42	YAPERMAG6	Y Aperture magnitude corrected to 5.7" diameter, AB
43	YAPERMAG6ERR	Y Error on Aperture magnitude (5.7" diameter), AB
44	YAPERMAGNOAPERCORR3	Y Fixed Aperture magnitude (2" diameter", AB)

45	YAPERMAGNOAPERCORR3ERR	Error in default extended source y aperture mag, 2.0 arcsec aperture
46	YAPERMAGNOAPERCORR6	Y Fixed Aperture magnitude (5.7" diameter, AB)
47	YAPERMAGNOAPERCORR6ERR	Error in extended source y aperture mag (5.7 arcsec aperture)
48	YERRBITS	Y SExtractor Flag
49	YCLASSSTAT	Y SExtractor Star/Galaxy classification (0-galaxy, 1-star)
50	YAUTOMAG	Extended source Y mag (SExtractor MAG_AUTO)
51	YAUTOMAGERR	Extended source Y mag error (SExtractor MAG_AUTO)
52	YHALFRAD	SExtractor half-light radius in Y band
53	JPETROMAG	J Petrosian magnitude (AB)
54	JPETROMAGERR	J Petrosian magnitude error (AB)
55	JAPERMAG3	J Aperture magnitude corrected to 2" diameter, AB
56	JAPERMAG3ERR	J Error on Aperture magnitude (2", diameter AB)
57	JAPERMAG6	J Aperture magnitude corrected to 5.7" diameter, AB
58	JAPERMAG6ERR	J Error on Aperture magnitude (5.7" diameter), AB
59	JAPERMAGNOAPERCORR3	J Fixed Aperture magnitude (2" diameter", AB)
60	JAPERMAGNOAPERCORR3ERR	Error in default extended source j aperture mag, 2.0 arcsec aperture
61	JAPERMAGNOAPERCORR6	J Fixed Aperture magnitude (5.7 diameter, AB)
62	JAPERMAGNOAPERCORR6ERR	Error in extended source j aperture mag (5.7 arcsec aperture)
63	JERRBITS	J SExtractor Flag
64	JCLASSSTAT	J SExtractor Star/Galaxy classification (0-galaxy, 1-star)
65	JAUTOMAG	Extended source J mag (SExtractor MAG_AUTO)
66	JAUTOMAGERR	Extended source J mag error (SExtractor MAG_AUTO)
67	JHALFRAD	SExtractor half-light radius in J band
68	HPETROMAG	H Petrosian magnitude (AB)
69	HPETROMAGERR	H Petrosian magnitude error (AB)
70	HAPERMAG3	H Aperture magnitude corrected to 2" diameter, AB
71	HAPERMAG3ERR	H Error on Aperture magnitude (2", diameter AB)
72	HAPERMAG6	H Aperture magnitude corrected to 5.7" diameter, AB
73	HAPERMAG6ERR	H Error on Aperture magnitude (5.7" diameter), AB
74	HAPERMAGNOAPERCORR3	H Fixed Aperture magnitude (2" diameter, AB)
75	HAPERMAGNOAPERCORR3ERR	Error in default extended source h aperture mag, 2.0 arcsec aperture
76	HAPERMAGNOAPERCORR6	H Fixed Aperture magnitude (5.7" diameter, AB)
77	HAPERMAGNOAPERCORR6ERR	Error in extended source h aperture mag (5.7 arcsec aperture)
78	HERRBITS	H SExtractor Flag
79	HCLASSSTAT	H SExtractor Star/Galaxy classification (0-galaxy, 1-star)
80	HAUTOMAG	Extended source H mag (SExtractor MAG_AUTO)
81	HAUTOMAGERR	Extended source H mag error (SExtractor MAG_AUTO)
82	HHALFRAD	SExtractor half-light radius in H band
83	KSPETROMAG	Ks Petrosian magnitude (AB)

84	KSPETROMAGERR	Ks Petrosian magnitude error (AB)
85	KSAPERMAG3	Ks Aperture magnitude corrected to 2" diameter, AB
86	KSAPERMAG3ERR	Ks Error on Aperture magnitude (2", diameter AB)
87	KSAPERMAG6	Ks Aperture magnitude corrected to 5.7 diameter, AB
88	KSAPERMAG6ERR	Ks Error on Aperture magnitude (5.7" diameter), AB
89	KSAPERMAGNOAPERCORR3	Ks Fixed Aperture magnitude (2" diameter", AB)
90	KSAPERMAGNOAPERCORR3ERR	Error in default extended source ks aperture mag, 2.0 arcsec
91	KSAPERMAGNOAPERCORR6	Ks Fixed Aperture magnitude (5.7" diameter", AB)
92	KSAPERMAGNOAPERCORR6ERR	Error in extended source ks aperture mag (5.7 arcsec aperture)
93	KSERRBITS	Ks SExtractor Flag
94	KSCLASSSTAT	Ks SExtractor Star/Galaxy classification (0-galaxy, 1-star)
95	KSAPERMAG	Extended source Ks mag (SExtractor MAG_AUTO)
96	KSAPERMAGERR	Extended source Ks mag error (SExtractor MAG_AUTO)
97	KSHALFRAD	SExtractor half-light radius in Ks band
98	PRIMARY_SOURCE	Defines whether a single source is detected twice due to adjacent tiles overlapping. PRIMARY_SOURCE=1 contains the more reliable photometry, and should be used when constructing a unique source catalogue.

The individual-tile catalogue format was derived from similar APM/SuperCOSMOS/INTWFC/CIRSI analyses that produced 32 4-byte parameters per detected object. This was first enhanced for WFCAM to an 80 4-byte parameter set to include extra parameters for flux estimation and error estimates, and this has now been further refined for the VIRCAM catalogues. The following tables cover the VIRCAM standard and further processing pipeline output catalogues, where for simplicity all derived parameters are stored as floating point numbers even though some of them are more naturally integers. See <http://casu.ast.cam.ac.uk/surveys-projects/vista/technical/catalogue-generation> for more information.

Table 8. Complete list of supplied catalogue columns for the sources lists released with the individual stacked paw-prints and tiles.

No	Name	Column Description
1	Seq No.	Running number for ease of reference, in strict order of image detections
2	Isophotal flux	Standard definition of summed flux within detection isophote, apart from detection filter is used to define pixel connectivity and hence which pixels to include. This helps to reduce edge effects for all isophotally derived parameters.
3	X coord	Intensity-weighted isophotal centre-of-gravity in X
4	Error in X	Estimate of centroid error
5	Y coord	Intensity-weighted isophotal centre-of-gravity in Y
6	Error in Y	Estimate of centroid error
7	Gaussian sigma	These are derived from the three general intensity-weighted second moments
8	Ellipticity	The equivalence between them and a generalised elliptical Gaussian
9	Position angle	Position angle of the isophote
10-17	Areal profile 1-8	Number of pixels above a series of threshold levels relative to local sky. Levels are set at T, 2T, 4T, 8T ... 128T where T is the threshold.

		These can be thought of as a radial profile. Note that for now, deblended, i.e. overlapping images, only the first areal profile is computed and the rest are set to -1 flagging the difficulty of computing accurate profiles for blended images this parameter is used to flag the start of the sequence of the deblended components by setting the first in the sequence to 0.
18	Peak height	In counts relative to local value of sky - also zeroth order aperture flux
19	Error in pkht	Error in Peak Height
20-45	Aperture flux 1-13 and error on aperture flux 1-13	<p>These are a series of different radii soft-edged apertures designed to adequately sample the curve-of-growth of the majority of images and to provide fixed-sized aperture fluxes for all images. The scale size for these apertures is selected by defining a scale radius $_FWHM$ for site+instrument. In the case of VIRCAM this “core” radius (r_{core}) has been fixed at 1.0 arcsec for convenience in inter-comparison with other datasets. A 1.0 arcsec radius is equivalent to 3.0 pixels for normal data. In 0.8 arcsec seeing an r_{core}-radius aperture contains roughly 75% of the total flux of stellar images.</p> <p>The aperture fluxes are sky-corrected integrals (summations) with a soft-edge (i.e. pro-rata flux division for boundary pixels). However, for overlapping images they are more subtle than this since they are in practice simultaneously fitted top-hat functions, to minimise the effects of crowding. Images external to the blend are also flagged and not included in the large radius summations.</p> <p>Starting with parameter 20 the radii are: $1/2 \times r_{core}$, $1/\sqrt{2} \times r_{core}$, r_{core}, $\sqrt{2} \times r_{core}$, $2 \times r_{core}$, $2\sqrt{2} \times r_{core}$, $4 \times r_{core}$, $5 \times r_{core}$, $6 \times r_{core}$, $7 \times r_{core}$, $8 \times r_{core}$, $10 \times r_{core}$, $12 \times r_{core}$</p> <p>We recommend using Aperture flux 3 if a single number is required to represent the flux for ALL images - this aperture has a radius of $r_{core} = 1$ arcsec.</p>
46	Petrosian radius	Petrosian radius as defined in Yasuda et al. 2001 AJ 112 1104
47	Kron radius	Kron radius as defined in Bertin and Arnouts 1996 A&A Supp 117 393
48	Hall radius	Hall image scale radius eg. Hall & Mackay 1984 MNRAS 210 979
49	Petrosian flux	Petrosian flux within circular aperture to $k \times r_p$ with $k=2$
50	Error in flux	Error on Petrosian flux
51	Kron flux	Flux within circular aperture to $k \times r_k$ with $k=2$
52	Error in flux	Error on Kron flux
53	Hall flux	Flux within circular aperture to $k \times r_h$ with $k=5$; alternative total flux
54	Error in flux	Error on Hall flux
55	Error bit flag	Bit pattern listing various processing error flags initially set to the no. of bad pixels within aperture of radius “ r_{core} ”- note this can be fractional due to soft-edged apertures
56	Sky level	Local interpolated sky level from background tracker
57	Sky rms	Local estimate of variation in sky level around image
58	Av conf	Average confidence level within default r_{core} aperture useful for spotting spurious outliers in various parameter selection spaces
		The following are accreted after standard catalog generation
59	RA	Right Ascension in radians (J2000)
60	Dec	Declination in radians (J2000)
61	Classification	Flag indicating most probable morphological classification: eg. -1 stellar, +1 non-stellar, 0 noise, -2 borderline stellar (Saturated images can be flagged by comparing the peak height + local sky with the SATURATE keyword in the header.)
62	Statistic	An equivalent $N(0,1)$ measure of how stellar-like an image is, used in deriving parameter 61 in a ‘necessary but not sufficient’ sense. Derived mainly from the curve-of-growth of flux using the well-defined

		stellar locus as a function of magnitude as a benchmark (see Irwin et al. 1994 SPIE 5493 411 for more details).
63	MJDoff	The number of minutes to be added to MJD_DAY in order to get the MJD of a given object. Hence for the i th object: $MJD_i = MJD_DAY + MJDoff_i / 1440.0$
64	Blank	Blank
65	Blank	Blank
66	Blank	Blank
67	Blank	Blank
68	Blank	Blank
69	Blank	Blank
70	Blank	Blank
71	Blank	Blank
72	Blank	Blank
73	Blank	Blank
74	Blank	Blank
75	Blank	Blank
76	Blank	Blank
77	Blank	Blank
78	Blank	Blank
79	Blank	Blank
80	Blank	Blank

Acknowledgements

The VIDEO Survey is described in Jarvis et al. 2013, MNRAS, 428, 1281 and any publications using the VIDEO data should reference this article.

Please use the following statement in your articles when using these data:

Based on data products from observations made with ESO Telescopes at the La Silla Paranal Observatory as part of the VISTA Deep Extragalactic Observations (VIDEO) survey, under programme ID 179.A-2006 (PI: Jarvis).

References

- Bertin E. & Arnouts S., 1996, ApJS, 117, 393
 Irwin M.J., et al., 2004, SPIE, 5493, 411
 Jarvis M.J., et al., 2013, MNRAS, 428, 1281
 Schlegel D.J., Finkbeiner D.P. & Davis M., 1998, ApJ, 500, 525
 Skrutskie M.F., et al., 2006, AJ, 131, 1163